

Reflection high-energy electron diffraction experimental analysis of polycrystalline MgO films with grain size and orientation distributions

R. T. Brewer^{a)} and Harry A. Atwater

Thomas J. Watson Laboratory of Applied Physics, California Institute of Technology, Pasadena, California 91125

J. R. Groves and P. N. Arendt

Superconductor Technology Center, Los Alamos National Laboratories, Los Alamos, New Mexico 87545

(Received 16 July 2002; accepted 11 October 2002)

Analysis of biaxial texture of MgO films grown by ion-beam-assisted deposition (IBAD) has been performed using a quantitative reflection high-energy electron diffraction (RHEED) based method. MgO biaxial texture is determined by analysis of diffraction spot shapes from single RHEED images, and by measuring the width of RHEED in-plane rocking curves for MgO films grown on amorphous Si₃N₄ by IBAD using 750 eV Ar⁺ ions, at 45° incidence angle, and MgO e-beam evaporation. RHEED-based biaxial texture measurement accuracy is verified by comparison with in-plane and out-of-plane orientation distribution measurements made using transmission electron microscopy and x-ray rocking curves. *In situ* RHEED measurements also enable the analysis of the evolution of the biaxial texture which narrows with increasing film thickness. RHEED-based measurements of IBAD MgO biaxial texture show that the minimum in-plane orientation distribution depends on the out-of-plane orientation distribution, and indicates that the minimum obtainable in-plane orientation on distribution is 2°. © 2003 American Institute of Physics. [DOI: 10.1063/1.1526156]

I. INTRODUCTION

Growth of biaxially textured MgO thin films is technologically interesting because it may provide a suitable path for silicon integration of many important single crystal-like perovskite oxide thin films on top of the amorphous dielectric thin films present at the back end of a typical integrated circuit fabrication process. This is accomplished by using ion beam-assisted deposition (IBAD) to create biaxially textured films (i.e., polycrystalline films with a preferred in-plane and out-of-plane grain orientation) on amorphous substrates. Film functionality often depends on control of both the out-of-plane grain orientation distribution [the full width at half maximum (FWHM) is designated as $\Delta\omega$] and in-plane grain orientation distribution (FWHM is designated as $\Delta\phi$). Some highly aligned biaxially textured oxide materials can exhibit similar functionality to single crystalline films. For example, biaxially textured superconductors such as YBa₂Cu₃O_{7-x} have been reported to have critical current densities approaching those of single crystalline films, while randomly oriented polycrystalline films exhibit much lower critical current densities.¹ Biaxially textured piezoelectric films with 90° domain rotations are also expected to have flexing characteristics similar to those of single crystalline piezoelectric films, while randomly oriented polycrystalline piezoelectric films experience significant degradation of translational range of motion. Incorporation of biaxially textured piezoelectric films with silicon integrated circuits would enable

new types of ferroelectric actuators for microelectrical mechanical systems (MEMS). Previous work has shown that piezoelectric materials like BaTiO₃ and Pb(Zr,Ti)O₃ can be deposited heteroepitaxially onto single crystal MgO (001)^{2,3} and even Si (001).⁴ However, conventional silicon integrated circuit processing employs extensive hydrogen passivation, which degrades ferroelectrics like Pb(Zr,Ti)O₃ and BaTiO₃. It is therefore desirable to monolithically integrate piezoelectric materials following integrated circuit fabrication. Wang *et al.* demonstrated that IBAD MgO grown on amorphous Si₃N₄ develops narrow biaxial texture in films only 11 nm thick.⁵ By eliminating the requirement for a pre-existing heteroepitaxial template, IBAD provides an opportunity to incorporate piezoelectric materials on top of amorphous dielectric films in silicon integrated circuits during the back-end processing.

The performance of piezoelectric MEMS is likely to depend on the biaxial texture inherited from the MgO substrate. Previous efforts to optimize the biaxial texture of IBAD MgO have been impeded by the *ex situ* nature of conventional biaxial texture analysis techniques [transmission electron microscopy (TEM) or x-ray diffraction (XRD)]. Because the biaxial texture develops within 11 nm of growth, XRD cannot resolve crystallographic texture unless the x-ray source has synchrotron brightness. For these same reasons, the IBAD biaxial texturing mechanisms are difficult to investigate. To circumvent these obstacles, we have developed a reflection high-energy electron diffraction (RHEED) based method for quantitative *in situ* biaxial texture analysis of MgO. RHEED has been previously used to analyze the out-

^{a)}Website: <http://daedalus.caltech.edu/~rhett/index.shtml>; electronic mail: rhett@its.caltech.edu

of-plane texture for CoCr alloys, assuming the grains were not large enough to affect the RHEED pattern.⁶ The small grain size of IBAD MgO films (as small as 10 nm) necessitate that we deconvolute the effects of grain size from the effects of out-of-plane orientation distribution for accurate texture distribution measurements. We also demonstrate the ability to measure the in-plane orientation distribution. Because RHEED is sensitive to films as thin as 3 nm thick, we have the capability of analyzing the biaxial texture development during the earliest stages of film growth.⁷ This analysis capability enables greater understanding of IBAD MgO biaxial texture development and how to optimize the MgO biaxial texture.

II. EXPERIMENTAL APPROACH AND MODEL-BASED ANALYSIS

Our RHEED-based biaxial texture analysis employs a previously reported kinematical electron scattering model.⁸ These calculations predict that spot shapes are sensitive to the film microstructure, as shown in Fig. 1(a). Diffraction spot width and height are inversely proportional to the effective grain size and electron penetration depth, respectively. The width of the diffraction spot in the direction perpendicular to the location of the through spot, the nondiffracted electron beam, is directly proportional to the out-of-plane grain orientation distribution ($\Delta\omega$). We therefore characterize RHEED patterns, whether calculated using a computer simulation or from an experiment, by cutting across the diffraction spots along the previously mentioned directions, and measuring the FWHM of these cuts, as shown in Fig. 1(b). We call this method “single image analysis.” All diffraction spots shown in Fig. 1(b) are analyzed simultaneously, and then compared to calculated RHEED pattern measurements using a lookup table. The lookup table was generated by calculating the RHEED pattern for all relevant combinations of effective grains size (4–25 nm), electron penetration depth (2.5–10 nm), and out-of-plane orientation distribution (0° – 20° FWHM), and measuring the FWHM of cuts across the six diffraction spots shown in Fig. 1(b) in the directions where the RHEED pattern is sensitive to electron penetration depth, grain size, and out-of-plane orientation distribution.

The effects of the in-plane orientation distribution on diffraction spot shapes are negligible, so the in-plane orientation distribution FWHM was set to 10° for lookup table calculations, which is a typical value for in-plane orientation distributions observed in IBAD MgO. Lookup table entries exist for all combinations of effective grain size, electron penetration depth, and out-of-plane orientation distribution, and contain the measurements of the FWHM of the cuts across each previously specified spot along the previously specified directions. The film effective grain size, electron penetration depth, and out-of-plane orientation distribution are determined by comparing the FWHM of experimental RHEED pattern diffraction spot cuts with the FWHM of the spot cuts in the lookup table. For each lookup table entry, the experimentally measured FWHM of each spot cut is subtracted from the lookup table FWHM of the same spot in the same direction. The differences between the experimental and lookup table measurements are then individually squared

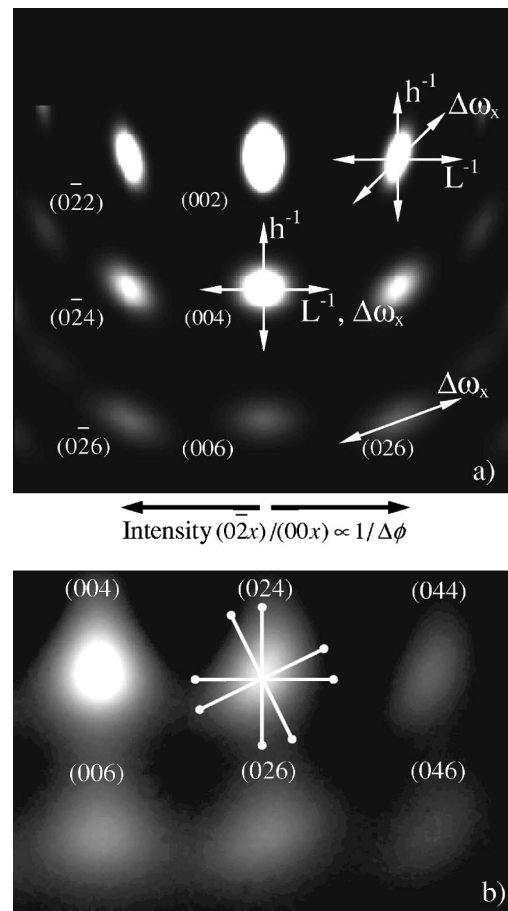


FIG. 1. RHEED images of MgO. (a) Simulated RHEED pattern of 20 keV electrons at 1.2° grazing incidence along [100] from well-textured polycrystalline MgO with effective lateral grain size $L=4$ nm, electron penetration depth $h=1$ nm, out-of-plane grain orientation distribution $\Delta\omega=7^\circ$, and in-plane orientation distribution $\Delta\phi=14^\circ$. The qualitative effects of these parameters upon the RHEED spot shapes and relative intensities are indicated. (b) Experimental RHEED image from IBAD MgO showing the diffraction spots that are simultaneously analyzed to measure effective grain size and out-of-plane orientation distribution. The diffraction pattern is characterized by measuring the diffraction spot widths along directions that are dependent on effective grain size, electron penetration depth, and out-of-plane orientation distribution. As an example, these directions are marked on the (024) diffraction spot.

before being added together to yield a total sum of the square errors measurement for that lookup table entry. The sum of the squared errors is calculated for every lookup table entry, and the microstructural parameters are determined as the simulated combination of electron penetration depth, effective grain size, and out-of-plane orientation distribution that yields the smallest sum of the squared errors. Even though the kinematical electron scattering calculations predict that the relative intensities of diffraction spots along the (00), (02), and (04) Bragg rods are correlated to the in-plane orientation distribution, it is not a very sensitive measurement. Therefore, RHEED in-plane rocking curves are used to measure the in-plane orientation distribution.

RHEED in-plane rocking curves are constructed by rotating the sample around the surface normal and recording the maximum intensity for each diffraction spot, minus the average background intensity, for each angle ϕ (the angle

between the nominal [100] zone axis and the projection of the incident electron beam on the sample surface). The resulting intensity distributions are characterized by the FWHM. To experimentally measure in-plane grain orientation distribution ($\Delta\phi$), the FWHM of RHEED in-plane rocking curves⁹ from the (024), (026), (044), and (046) diffraction spots are measured simultaneously and compared to the FWHM of calculated in-plane rocking curves in another lookup table. As for the single image analysis, a lookup table was generated by calculating the FWHM of diffraction spot in-plane RHEED rocking curves for all relevant film parameter combinations, i.e., effective grain size (4–25 nm), out-of-plane orientation distribution (0°–20° FWHM), and in-plane orientation distribution (0°–30° FWHM).

In-plane rocking curve FWHM was calculated to be independent of the electron penetration depth, so it was set to 5 nm, the value most often measured using single image analysis at this electron energy and incidence angle. Each lookup table entry was indexed by its unique combination of the relevant film parameters (grain size, out-of-plane orientation distribution, and in-plane orientation distribution) and contained the FWHM of the rocking curves from the (024), (026), (044), and (046) diffraction spots. The in-plane orientation distribution is determined by searching the lookup table for the simulation that has RHEED in-plane rocking curves that most closely match the experimental rocking curves for all four diffraction spots. The FWHM of the in-plane rocking curves are highly correlated with the in-plane orientation distribution, however, the rocking curve FWHM is also convoluted with the effective grain size and out-of-plane orientation distribution. Therefore, to accurately measure in-plane orientation distribution using in-plane rocking curves, the effective grain size and out-of-plane orientation distribution is first measured using single image analysis as described above. The subsequent comparison between the experimental and simulated FWHM of the RHEED in-plane rocking curves in the lookup tables are restricted to simulations with the effective grain size and out-of-plane orientation distribution measured using single image analysis.

Experimental RHEED in-plane rocking curves and single image analyses were performed on 5- to 11-nm-thick IBAD MgO films. MgO was deposited, at room temperature, on amorphous Si₃N₄ by electron beam evaporation at deposition rates ranging from 1.7 to 3.1 Å/s, as measured by a quartz crystal monitor. Ion irradiation during MgO growth was carried out with 750 eV Ar⁺ ions at 45° incidence angle. Ion/MgO flux ratios were varied between 0.33 and 0.58. A single crystal of MgO was also analyzed for reference. Optimal film thickness was determined by monitoring the (004) diffraction peak intensity.¹⁰ RHEED measurements were done at 25 kV and 2.6° incidence angle. Bragg spots along the (00), (02), and (04) Bragg rods, as shown in Fig. 1(b) were used in the RHEED analysis. A 16 bit, 1024×1024 pixels CCD camera provided adequate dynamic range to simultaneously observe all necessary spots and to spatially resolve spot shapes for single image analysis. Before attempting single image analysis, the diffuse background was reduced by subtracting the Si₃N₄ substrate RHEED image from the IBAD MgO RHEED pattern. This procedure was

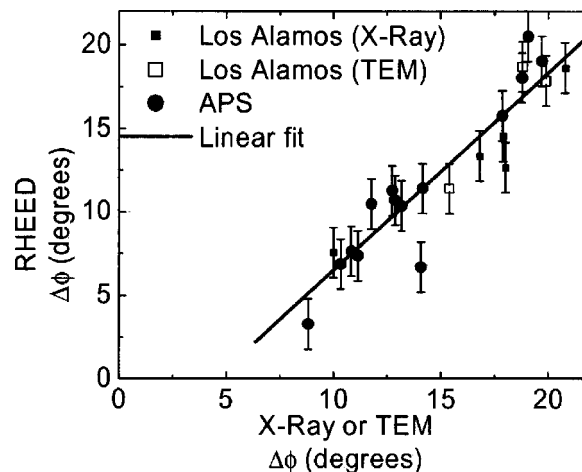


FIG. 2. In-plane orientation distribution ($\Delta\phi$) measured by RHEED analysis versus TEM or XRD measurements. X-ray rocking curves were collected using either a rotating anode source at Los Alamos or synchrotron radiation from the APS. The error bars originate from limitations in deconvoluting the effects of out-of-plane orientation distribution and grain size measurements using RHEED.

necessary to resolve weak diffraction spots and to reduce shape distortion caused by the diffuse background.

Biaxial texture was also measured with either TEM or XRD to evaluate the accuracy of RHEED based measurements. The grazing incidence geometry of in-plane rocking curves enabled the use of either a rotating anode source or the Advanced Photon Source (APS) synchrotron to measure in-plane orientation distributions. However, out-of-plane orientation measurements of IBAD MgO layers required synchrotron radiation for the out-of-plane x-ray rocking curves. Even with the APS synchrotron radiation, the x-ray rocking curves did not provide reliable out-of-plane orientation distribution measurements for 8-nm-thick MgO samples with the broadest out-of-plane distributions (>11°).

III. RESULTS AND DISCUSSION

A. RHEED-based measurement validation: In plane orientation distribution

The in-plane orientation distributions measured using RHEED-based analysis is compared to measurements from TEM or x-ray scattering in Fig. 2. The data are well represented by a linear fit, demonstrating that the RHEED-based method successfully measures the in-plane orientation distribution. There are many possible sources of deviation from the straight line. The RHEED measurements require the deconvolution of the effective grain size and out-of-plane orientation distribution from the in-plane distribution. Errors in measurements of the effective grain size and out-of-plane orientation distribution therefore produce errors in the in-plane orientation distribution measurement. There is also a convolution between the measurement of effective grain size and out-of-plane orientation distribution such that an error in one measurement is compensated by an error in the other measurement. Reasonable errors for measurements of effective grain size and out-of-plane orientation distribution (± 1 nm and $\pm 1^\circ$, respectively) yield a total in-plane measure-

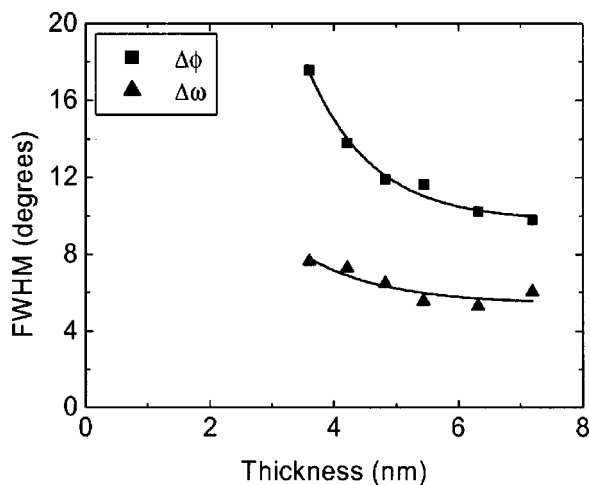


FIG. 3. In-plane ($\Delta\phi$) and out-of-plane ($\Delta\omega$) orientation distribution for IBAD MgO growth as a function of film thickness measured using RHEED. The lines are a fit to the data.

ment error of $\pm 1.5^\circ$, represented by the error bars in Fig. 2. Additional deviations from linear dependence originate in different sample-to-sample growth conditions that were used to produce films with the wide range of in-plane orientation distributions observed in Fig. 2. Measurements of IBAD MgO in-plane orientation distribution as a function of film thickness demonstrate that the in-plane orientation distribution decreases with increased film thickness, as illustrated in Fig. 3. We have also observed that the rate at which the in-plane distribution decreases depends on the ion/MgO flux ratio. TEM and x-ray scattering techniques probe the biaxial texture in a scattering volume that spans the entire thin film, measuring the film's average orientation distribution, while RHEED measurements are more surface sensitive. Therefore, the in-plane orientation distribution measured by RHEED, a surface sensitive measurement, is not expected to directly correspond to the x-ray measurement, which probes the entire film thickness. With 750 eV Ar^+ ion bombardment, the first 3 nm of the IBAD MgO film are amorphous. However, this layer yields a biaxially textured film out of the amorphous matrix through solid phase crystallization.⁷ The first measurable RHEED patterns reveal that the initial in-plane orientation distributions are very broad, but they narrow as the film thickens until reaching an optimal alignment. The difference between the initial and optimal in-plane orientation distribution measurements is typically on the order of 10° under these growth conditions. Depending on the thickness of the final film, the difference between the average and surface in-plane orientation distribution will be different, causing another possible source of deviation from the linear fit in Fig. 2.

Optimal biaxial texture under specific growth conditions is achieved by growing the film until the (004) diffraction spot reaches its maximum intensity.¹⁰ Integrating the measured in-plane orientation distribution in Fig. 3 over the entire film thickness yields an average film in-plane orientation distribution about 2.5° broader than the surface in-plane orientation distribution. This is consistent with the offset between the in-plane orientation distribution measurements

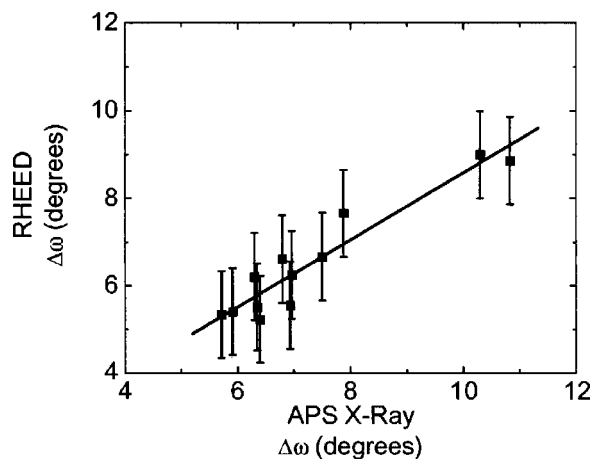


FIG. 4. Out-of-plane orientation distribution ($\Delta\omega$) measured using RHEED and synchrotron X-ray out-of-plane rocking curves. The line is a linear fit to the data.

based on RHEED analysis and the x-ray or TEM analysis. The magnitude of this offset depends on the thickness of the film when growth was stopped, as well as on growth conditions such as ion/MgO flux ratio.

Despite the expected differences between the surface sensitive and bulk measurement methods, as well as the inherent limitations of the RHEED measurements because of convolution with effective grain size and out-of-plane distribution measurements, the comparison between RHEED and x-ray or TEM measurements is well represented by a linear fit. Not only does this analysis illustrate that RHEED can be used for *in situ*, quantitative in-plane orientation distribution measurements, it also highlights that the RHEED-based method yields more accurate estimates of surface biaxial textures than does XRD.

B. RHEED-based measurement validation: Out-of-plane orientation distribution

X-ray measurement of in-plane orientation distributions can be done with a rotating anode source because the grazing incidence geometry creates a relatively large scattering volume even for very thin films. Out-of-plane orientation distribution, measured with theta rocking curves, required synchrotron radiation to collect enough signal for reliable measurements. Even with the brightness of the 33ID-D undulator beamline at the APS synchrotron, which produced 3.0×10^5 counts per second (cps), some IBAD MgO films which yielded measurable in-plane rocking curves did not yield out-of-plane rocking curves with measurable peaks. RHEED measurements of out-of-plane orientation distribution are plotted in Fig. 4 against measurements from the same samples made using x-ray rocking curves at APS. The error bars on the RHEED measurements result from uncertainties in the deconvolution of effects from grain size and electron penetration depth broadening of the RHEED pattern from effects caused by the out-of-plane orientation distribution. As with the in-plane measurements, we expect a difference between surface sensitive RHEED measurements and bulk sensitive x-ray measurements. Figure 3 shows that *in*

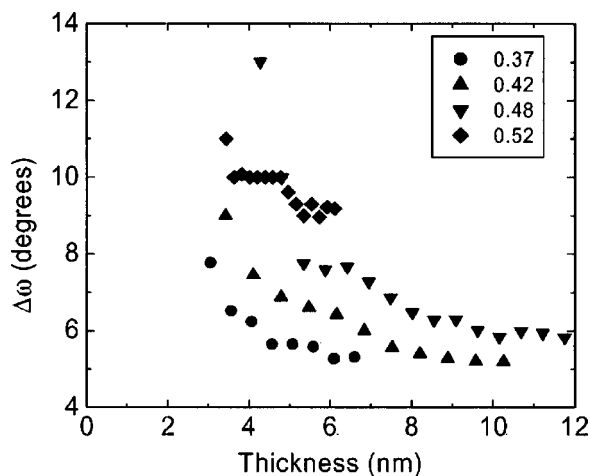


FIG. 5. *In situ* RHEED measurements of out-of-plane orientation distribution ($\Delta\omega$) as a function of film thickness for ion/MgO flux ratios from 0.37 to 0.52.

situ RHEED measurements of out-of-plane orientation distribution reveal that the out-of-plane distribution improves as the film grows, similar to the narrowing of the in-plane distribution with increasing film thickness. By integrating the RHEED out-of-plane distribution measurements over the film thickness, the average out-of-plane distribution is found to be approximately 1° broader than the surface measurement. This offset is consistent with the offset between the RHEED and x-ray measurements observed in Fig. 4.

C. Biaxial texture as a function of ion/MgO flux ratio measured using RHEED

RHEED-based biaxial texture measurement method provides information not measurable via x-ray scattering and facilitates measurements of biaxial texture, providing insight into biaxial texture development. One of the powerful aspects of RHEED-based analysis is the real-time acquisition of out-of-plane texture measurements. Figure 5 shows the out-of-plane orientation distribution measured from IBAD MgO as a function of film thickness and ion/MgO flux ratio. As illustrated previously in Fig. 3, during IBAD the out-of-plane orientation distribution narrows as the film grows. At 0.52 ion/MgO flux ratio (Ar^+ energy of 750 eV), the deposition condition is close to producing zero net growth because of ion sputtering, and therefore results in increased ion damage to the MgO film. Decreasing the ion/MgO flux ratio from 0.52 to 0.37 reduces the ion damage, resulting in more rapid narrowing of the out-of-plane orientation distribution as the film grows. Each data point in Fig. 5 was collected during IBAD MgO growth by taking a one second exposure time image of the RHEED pattern, the points being separated by 3 s of growth. The low noise levels from point to point show that the measurement technique is stable and reproducible. Using x rays to obtain out-of-plane orientation distributions as a function of film thickness would require stopping the growth at each thickness interval and performing an out-of-plane rocking curve. Using the 33ID-D beamline with 2.9×10^5 cps, the out-of-plane rocking curve for a 4 nm MgO film, with an out-of-plane FWHM of 7° , took over 30 min to

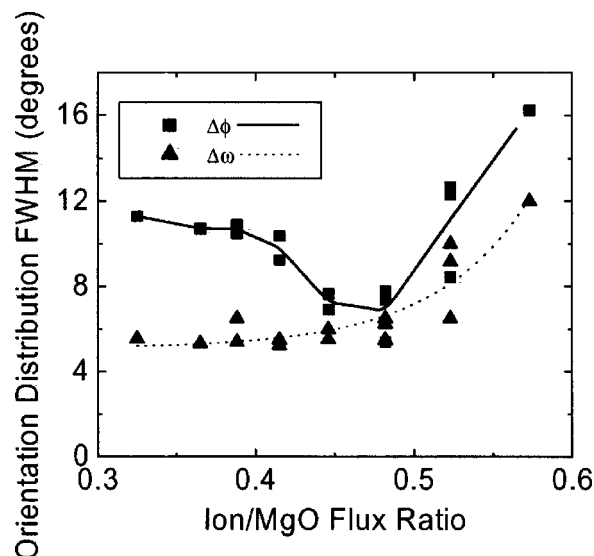


FIG. 6. Optimal in-plane ($\Delta\phi$) and out-of-plane ($\Delta\omega$) orientation distributions for IBAD MgO growth with 750 eV Ar^+ ions as a function of ion/MgO molecule flux ratio. Measurements were performed using RHEED based analysis and the lines are fits to the data.

resolve. The real-time RHEED measurements have the added advantage of being more surface sensitive than XRD, allowing for a more accurate picture of the out-of-plane texture evolution as a function of film thickness.

Simultaneous RHEED-based measurements of both the in-plane and out-of-plane orientation distribution yield insights into the limitations of in-plane texturing through IBAD. Figure 6 shows the dependence of the optimal in-plane and out-of-plane orientation distributions as a function of ion/MgO flux ratio. The optimal in-plane orientation distribution as a function of ion/MgO flux ratio has been previously measured by Wang for 700 eV Ar^+ ion bombardment.¹⁰ We observe a similar trend for the dependence of in-plane distribution with ion/MgO flux ratio using RHEED-based measurements as was observed using XRD; however, the efficiency of the RHEED method allowed us to more finely resolve the dependency of the in-plane distribution on ion/MgO flux ratio and also measure the out-of-plane orientation distribution simultaneously. We observe two regimes of biaxial texturing: at low ion/MgO flux ratio the out-of-plane orientation distribution is constant and the in-plane orientation distribution gets narrower as the ion/MgO flux ratio increases, while at high ion/MgO flux ratios the out-of-plane orientation distribution is constant and the in-plane orientation distribution gets narrower as the ion/MgO flux ratio increases, while at high ion/MgO flux ratios the out-of-plane orientation distribution broadens with increasing ion/MgO flux ratio and is accompanied by a broadening of the in-plane orientation distribution.

High temperature physical vapor deposition of MgO on amorphous SiO_2 favors nucleation with a (001) fiber texture;¹¹ however, at room temperature we have not observed a strong out-of-plane texture without ion bombardment. The energy from the ion bombardment must be sufficient for the MgO to grow in the preferred [001] out-of-plane orientation. Ressler *et al.* proposed that ion induced in-plane

alignment results from anisotropic grain damage, where the grains with the most damage resistant planes are oriented toward the axis of the incoming ion flux.¹² For IBAD MgO, the (101) planes are found to orient toward the Ar⁺ ion bombardment. At low ion/MgO flux ratios, the film has enough energy to select the preferred (001) out-of-plane texture, but does not have enough ion bombardment to efficiently select the in-plane orientation of every crystal, resulting in a broad in-plane orientation distribution. As the ion/MgO flux ratio increases to the optimal ratio, between 0.45 and 0.48 for 750 eV Ar⁺ ion bombardment, the out-of-plane orientation distribution stays constant, while the increase in ion bombardment more efficiently selects the crystals with the (101) plane oriented toward the ion bombardment, until the in-plane orientation distribution is within 2° of the out-of-plane distribution. Once the ion/MgO flux ratio increases past the optimal conditions, ion damage cause the out-of-plane texture to broaden. A MgO crystal that has been rotated out-of-plane about the *x*-axis, the direction of the ion bombardment projected onto the plane of the substrate, misorients the (101) plane away from the Ar⁺ ions. However, a subsequent in-plane rotation, a rotation about the axis perpendicular to the substrate, can be used to restore the (101) plane to directly face the incident ions. As the out-of-plane distribution broadens, the distribution of in-plane rotations to realign the (101) directions along the axis of the incoming ion bombardment also broadens. The in-plane orientation distribution achievable with IBAD is limited by the out-of-plane orientation distribution. These experiments indicate that the minimum in-plane orientation distribution achievable for IBAD MgO with 750 eV Ar⁺ ion bombardment is 2°, which could only be obtained if the out-of-plane texture is perfectly aligned.

IV. CONCLUSION

We have developed a RHEED-based method for quantitative biaxial texture measurement of MgO. Comparison between biaxial texture measurements made using RHEED and synchrotron XRD confirm that *in situ* RHEED analysis yields quantitative measurements of both in-plane and out-of-plane grain orientation distribution. The systematic offsets between RHEED analysis and x-ray measurements of biaxial texture, coupled with evidence that biaxial texture improves with increasing film thickness, indicates that RHEED is a superior technique for probing surface biaxial texture. We have used RHEED to observe that the biaxial texture nucleates with a relatively broad orientation that improves as the

film thickness increases to an optimal level. We have also seen that the IBAD in-plane orientation mechanism limits the in-plane alignment due to the out-of-plane orientation distribution. We have found that the minimum in-plane orientation distribution requires perfect out-of-plane alignment, and that for 750 eV Ar⁺ IBAD MgO the optimal in-plane orientation distribution achievable is approximately 2° FWHM. RHEED simulations of other biaxially textured cubic materials like BaTiO₃ exhibit similar dependence on biaxial texture as seen in MgO, indicating that this method should be generally applicable to cubic materials. Weak scattering of MgO and rapid biaxial texture development make investigation of IBAD biaxial texture development difficult with *ex situ* XRD. The surface sensitivity and *in situ* nature of RHEED provides novel information about biaxial texture development and will facilitate rapid investigation of biaxial texturing mechanisms and biaxial texture optimization.

ACKNOWLEDGMENTS

The authors would like to thank J. F. Whitacre and P. Zschack for assistance with synchrotron measurements, as well as L. Emmert and P. C. Yashar for grazing incidence XRD measurements of IBAD MgO in-plane orientation distribution. This work was supported by the DARPA VIP III program and ARO MURI Grant No. DAAD19-01-1-0517. Use of the APS synchrotron was supported by the U.S. Department of Energy, Office of Science, Office of Basic Energy Sciences, under Contract No. W-31-109-Eng-38.

¹X. D. Wu *et al.*, Appl. Phys. Lett. **67**, 2397 (1995).

²W. J. Lin, T. Y. Tseng, H. B. Lu, S. L. Tu, S. J. Yang, and I. N. Lin, J. Appl. Phys. **77**, 6466 (1995).

³N. Wakiya, K. Kuroyanagi, Y. Xuan, K. Shinozaki, and N. Mizutani, Thin Solid Films **357**, 166 (1999).

⁴R. A. McKee, F. J. Walker, and M. F. Chisholm, Phys. Rev. Lett. **81**, 3014 (1998).

⁵C. P. Wang, K. B. Do, M. R. Beasley, T. H. Geballe, and R. H. Hammond, Appl. Phys. Lett. **71**, 2955 (1997).

⁶D. Litvinov, J. K. Howard, S. Khizroev, H. Gong, and D. Lambeth, J. Appl. Phys. **87**, 5693 (2000).

⁷R. T. Brewer and H. A. Atwater, Appl. Phys. Lett. **80**, 3388 (2002).

⁸J. W. Hartman, R. T. Brewer, and Harry A. Atwater, J. Appl. Phys. **92**, 5133 (2002).

⁹R. T. Brewer, J. W. Hartman, J. R. Groves, P. N. Arendt, P. C. Yashar, and H. A. Atwater, Appl. Surf. Sci. **175**, 691 (2001).

¹⁰C. P. Wang, Ph.D. Thesis, Stanford University, 1999.

¹¹J. S. Lee, B. G. Ryu, H. J. Kwon, Y. W. Jeong, and H. H. Kim, Thin Solid Films **354**, 82 (1999).

¹²K. G. Ressler, N. Sonnenberg, and M. J. Cima, J. Am. Ceram. Soc. **80**, 2637 (1997).